Characterization of Two Secondary Optics for a Fresnel Mirror

Daniela Fontani, David Jafrancesco, Franco Francini, Paola Sansoni
CNR-INO Istituto Nazionale di Ottica, Largo E. Fermi, 6 – Firenze - 50125 – Italy
Phone: +39-055-23081; Fax: +39-055-2337755; Email: daniela.fontani@ino.it

Abstract

The advantage of this laboratory optical characterization is to reproduce under controlled conditions an existing solar plant of Fresnel mirror type. The plant has 20 identical plane mirrors that concentrate the sunlight toward the secondary optics, which focuses it on the receiver. The procedure consists in performing the tests separately simulating the illumination of each plane mirror, finally combining the measured results to obtain collection efficiency and concentration factor of the entire solar plant. Two alternative secondary optics, a prismatic lens and a reflective concentrator, were optically tested to compare their behaviour. The total collection efficiency is similar, while the concentration factor is higher for the prismatic lens. Since the receiver is a photovoltaic device, a key aspect to be studied is the uniformity of receiver lighting: the power density measured in the image plane of the secondary optics evidences lateral zones of uneven lighting.

Keywords: secondary optics, Fresnel mirror, optical measurement, solar concentration

1. Analysis of the system

Two secondary concentrators were designed and realized for an actual solar concentration plant based on the principle of the Fresnel mirror [Abbas et al. 2012a, 2012b; El Gharbi et al. 2011; Fernandez-Garcıa et al. 2010; Kalogirou, 2004; Mills and Morrison, 2000; Singh et al. 1999; Winston et al. 2005]. The optical component is illuminated by 20 plane mirrors of equal size (50 mm x 1000 mm) that reflect the solar rays under various angles depending on the sunrays' inclination and on the relative positions of mirror and receiver [Fontani et al. 2015]. The secondary collector should then concentrate the solar light on a rectangular receiver of dimensions 50 mm x 10 mm [Fontani et al. 2015]. The secondary optics is placed as near as possible to the receiver to improve the collection efficiency, reduce the dimensions and avoid undesired shadow effects.

Several optical measurements and tests were effectuated on the implemented secondary concentrators. The tested optical components are a prismatic lens and a reflective concentrator [Abbas et al. 2012a, 2012b; El Gharbi et al. 2011; Fernandez-Garcıa et al. 2010; Kalogirou, 2004; Mills and Morrison, 2000; Singh et al. 1999]. The two elements are quite different because the working principle of the prismatic lens is based on refraction, while the other optics is based on reflection. The purpose of the laboratory tests is to study and characterize the optical properties and behaviour of the secondary optics in order to decide which is more suitable for improving the performance of the system. The two optical systems are compared in terms of collection efficiency and concentration factor, simulating the illumination arriving from the 20 mirrors at noon. In addition some image acquisitions are effectuated on the plane where the receiver will be placed, for a qualitative analysis of the illumination produced by the secondary optics on the receiver.

Tests and measurements are performed separately simulating the illumination of each plane mirror, being impossible to illuminate the samples in laboratory utilising 20 sources from different directions. The next phase is the data elaboration, for which it was chosen to perform the analysis at noon (as representative position, but the mirrors constantly move during the day). At noon the study can consider only 10 mirrors, exploiting the symmetry of the plant, and at noon there should be the maximum output of the solar plant. Hence it is interesting to compare the secondary optics behaviour in this particular moment of the day.

Angular aperture and incidence angle of the beam are the main factors that influence the collection efficiency of the secondary concentrator [Fontani et al. 2015]. Referring to Fig. 1, for the i-th mirror, the relevant parameters

doi:10.18086/swc.2017.18.06 Available at http://proceedings.ises.org

are:

- d: distance between mirrors line and receiver input (1000 mm).
- x_i: mirror position relative to the origin (fixed at the junction between the receiver normal passing through its centre and the mirrors line); measured positive to the right and negative to the left.
- D_i: distance between receiver centre and mirror centre.
- $\theta(t)$: sunlight incidence angle; measured from the normal to the mirrors line.
- $i_i(t)$: incidence angle of sunlight on the mirror; measured from the normal to the mirror.
- $\beta_i(t)$: tilt of the mirror; measured relative to the mirrors line.
- α_i: angle of the reflected beam; measured from the line of the mirrors.
- α'_i: incidence angle of the beam reflected on the receiver.

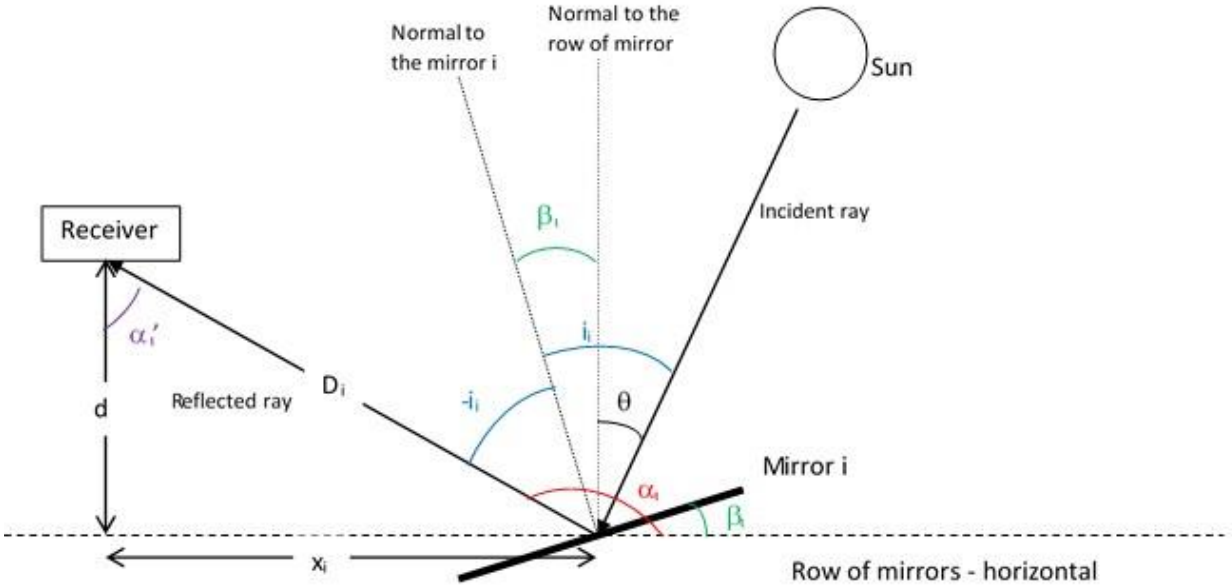

Fig. 1 – How the sunray is reflected by the primary system.

The sign of the angles is positive measuring counter-clockwise and negative measuring them clockwise.

For a given mirror, the angles i, β_i and θ are time dependent, while α_i must be constant to direct the beam toward the receiver. Referring to Fig. 1, the angles $i_i(t)$, $\theta(t)$, $\beta_i(t)$ and α_i are linked by 4 equations; so knowing α_i' (from the system geometry) and $\theta(t)$ (from the time of the day) α_i, $i_i(t)$, $\beta_i(t)$ can be derived [Fontani et al. 2015].

The collection efficiency of the receiver depends on how it is illuminated. For a single mirror the collection efficiency is defined as:

$$\eta_i\left(\alpha'_i, A_{eff,i}\right) = \frac{P_{out,i}(t)}{P_{in,i}(t)} \quad (1)$$

where $P_{out,i}(t)$ is the output power exiting from the receiver, and $P_{in,i}(t)$ the input power; α_i' is the entrance angle and $A_{eff,i}$ is the effective area of the beam entering into it. The input power is given by

$$P_{in,i}(t) = \bar{p}_i(t) \cdot A_{eff,i}(t) \quad (2)$$

where $\bar{p}_i(t)$ is the average power density of the beam at the receiver input.

The total collection efficiency (considering the contributions of all the mirrors) is

$$\eta = \frac{\sum_{i=1}^{20} P_{out,i}(t)}{\sum_{i=1}^{20} P_{in,i}(t)} \quad (3)$$

The concentration factor C_i for the i-th mirror is defined as:

$$C_i = \eta_i \frac{A_{in}^R}{A_{out}^R} \quad (4)$$

where A_{in}^{R} and A_{out}^{R} are respectively the physical area of receiver input and of receiver output.

Finally the total concentration factor C is given by:

$$C = \eta \frac{A_{in}^{R}}{A_{out}^{R}} \quad (5)$$

2. Measurement setup and procedure

The optical measurements are performed in a laboratory setup based on a solar divergence collimator, which produces a beam with solar divergence [Fontani et al. 2013]. Source, test sample and sensor are the principal components of the measurement system employed to optically characterize the samples of secondary collector. The scheme of the measurement set-up is reported in Fig. 2, with the pictures of the actual components as they are mounted on the optical table in laboratory.

The white beam emitted by the illuminator is angularly homogenized in the integrating sphere and comes out from the exit aperture of the sphere. Then the light is reflected by the collimation mirror, which generates a solar divergence beam. Suitable screens, to obtain a beam with dimensions adapted to illuminate the sample under test, finally cut this beam. The combination of the size of the sphere aperture with the focal length of the spherical mirror (collimation mirror) produces a uniform beam with solar divergence [Fontani et al. 2013].

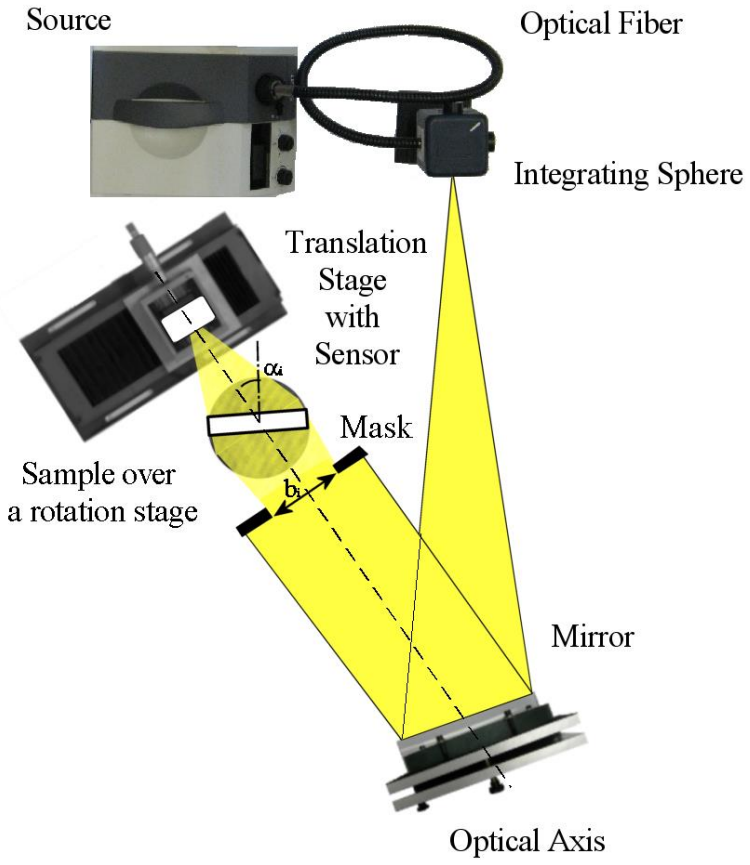

Fig. 2 – The optical system to test the secondary collectors.

The two secondary collectors examined are a prismatic lens and a reflective concentrator, specifically designed for the solar collection system of Fresnel mirror type.

The optical tests are executed with a reproducible procedure, identical for the two types of secondary optics. The final aim of this procedure of sample alignment and displacements is to reproduce the working conditions at noon

of the actual solar plant for which the secondary optics was developed.

Each examined sample is placed on a platform allowing rotation and translation with elevated precision and stability. The rotator has sensitivity of 0.025° and it permits to vary the incidence angle of the beam coming from the mirror. The micrometric translator allows to correct for the small difference between the rotation axis and the entrance of the secondary optics, so that the latter is always at the centre of the beam.

The acquisitions are of two types: photodiode measurements to obtain the collection efficiency or image acquisitions with a CMOS camera to know the light distribution in the image plane. The photodiode scan is a quantitative assessment, while the CMOS camera acquisition gives only qualitative information.

The main sensor is a photodiode with squared sensitive area of sizes 1 mm x 1 mm. The detector is mounted on a micrometric XY translating system, which allows to perform two-dimensional scans in a vertical plane (perpendicular to the optical axis, indicated in Fig. 2). Typically the examined vertical plane is the image plane of the secondary optics, where the optical design foresees that the collector creates its image. For these concentrators the photovoltaic (PV) receiver is placed in this plane and obviously the region of interest corresponds to the area of the receiver. The photodiode is connected to an amplifier, and the total amount of focused light, obtained by photodiode measurements, is used to calculate collection efficiency and concentration factor.

In addition to the photodiode scans, some image acquisitions are performed using a CMOS camera to know the light distribution in the image plane examined by the photodiode scans. The CMOS camera has sensitive area of size 7.74 mm x 10.51 mm. The camera is displaced with the same translation system used with the photodiode. The purpose is to assess the power density of the light focused on the receiver plane. This measurement gives information about uniformity of receiver illumination, which is a key parameter for obtaining the maximum conversion by the PV receiver.

A devoted LabVIEW program manages scansion and elaboration of measured signals for both sensors, allowing to select area and pitch of the scan. The mapping of the region of interest is automatically handled by this LabVIEW program that provides to move the shifters and to acquire the signal of the used sensor.

For the collection efficiency assessment with photodiode the procedure steps are listed below.

1) For a given time *t* the mirrors inclinations β_i for $\theta(t) = 0$ are known, consequently are obtained the angles α'_i of beam incidence on the receiver (10 in total, the other 10 correspond to $-\alpha'_i$), and the beam limiter widths.

2) Firstly a reference measurement is executed: the photodiode axis is aligned with the direction of the incident beam. It is performed a mapping of the beam incident on the receiver. The scanning is made on a plane perpendicular to the beam direction without the secondary optics.

3) The secondary optics is mounted, it is rotated up to the angle α'_i and the limiter opening is regulated.

4) Placing the photodiode in the measurement plane, the illuminated area is scanned to obtain a map, aligning the scan plane with the hypothetical plane of the PV cell. For the reflection concentrator, the detector is placed in the vicinity of the exit aperture. For the lenses, the detector is placed on the working plane, 50 mm from the rear surface of the lens. The shifters are moved with steps of 1 mm x 1 mm, in this way a direct and complete mapping of the image, with resolution limited by the detector size, is obtained.

5) steps 3) and 4) of the measurement procedure are repeated for all α'_i.

For the acquisition of images with CMOS camera the procedure is identical to the previous one, with the exclusion of the reference measurement, which is not needed in this type of acquisition since it is not a quantitative measurement. The scanning steps are in agreement with the CMOS sensor dimensions.

3. Data elaboration and results

The photodiode acquisitions are elaborated to calculate collection efficiency and concentration factor of the examined optical component.

The result of a scan with the photodiode is a two-dimensional matrix with dimension corresponding to the number of sampled points, and whose elements are the photodiode output current, which is proportional to the incident power. Since the sensitive area of the photodiode is 1 mm^2, these values can be considered as the power density

per mm^2.

The collection efficiency of the receiver is calculated using equations Eq. (1), Eq. (2) and Eq. (3). $P_{in,i}$ is given by Eq. (2), in which $\bar{p}$ is calculated by averaging the values of the scan on the incident beam. The effective area is rectangular: $A_{eff,i} = a \cdot b_i$. The receiver is always fully illuminated in the vertical direction, so a is constant for each measurement. The horizontal dimension (b_i) must be accurately calculated considering the projection (of length $l_{eff,i}$) of the receiver side (of length L_R) on the plane orthogonal to the beam axis [Fontani et al. 2015]. Each plane mirror (of length L_M) in the horizontal direction is seen with a length $L'_{eff,i}$, obtainable considering the projection effect and the beam divergence enlargement [Fontani et al. 2015].

Hence there are different situations of illumination. The receiver is fully illuminated (b_i data in bold in Tables 1-2) or it is partially illumined (b_i data in italics in Table 1). When it is entirely lighted $L'_{eff,i} > l_{eff,i}$ and $b_i = l_{eff,i}$, while in case of partial illumination $L'_{eff,i} < l_{eff,i}$ and $b_i = L'_{eff,i}$ [Fontani et al. 2015]. These quantities are visualized in Fig. 3.

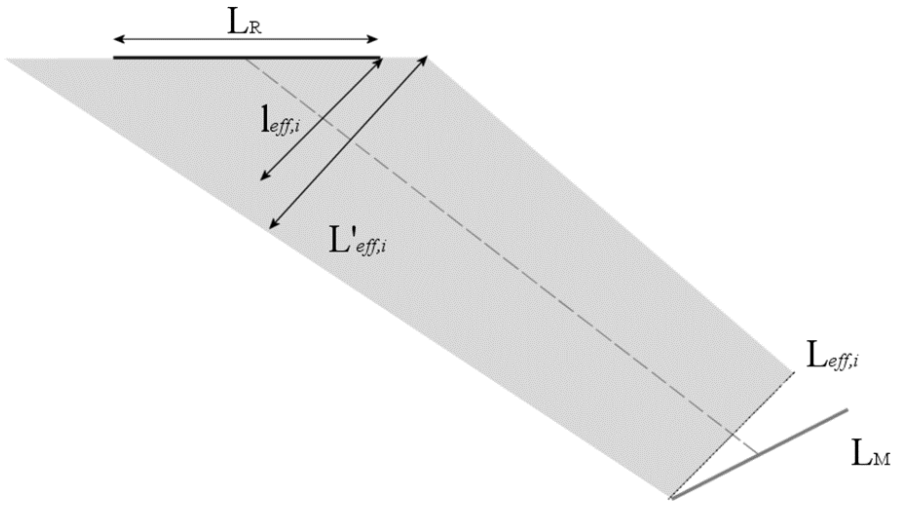

Fig. 3 – Effects on the beam.

Table 1 presents the measurement results for a reflection concentrator; whilst Table 2 reports the results measured on two samples of prismatic lens (denominated Lens1 and Lens2). The columns refer to: mirror tilt with respect to the mirrors line (β_i), incidence angle of the beam reflected on the receiver (α_i'), horizontal size of the effective area (b_i), and effective area ($A_{eff,i}$). The vertical size of the effective area is a.

From Table 1 it is clear that for the reflection concentrator there are some angles for which the beam does not completely enter in the receiver; in these cases the light collection is limited by the size of the receiver and not by the beam itself.

β_i (°)	α_i' (°)	b_i (mm)	$A_{eff,i}$ (mm^2)
0.759	1.518	**58.72**	2819
2.273	4.546	**58.69**	2817
3.774	7.548	**58.62**	2814
5.254	10.508	**58.52**	2809
6.707	13.414	*58.36*	2801
8.126	16.252	*57.60*	2765
9.504	19.008	*56.73*	2723
10.839	21.678	*55.76*	2676
12.126	24.252	*54.70*	2626
13.363	26.726	*53.59*	2572

Table – Effective area of the beam entering in the reflection concentrator as a function of the entrance angle, for a = 48 mm.

β_i (°)	α_i' (°)	b_i (mm)	$A_{i,eff}$ (mm^2)
0.759	1.518	**58.72**	2936
2.273	4.546	**58.69**	2934
3.774	7.548	**58.62**	2931
5.254	10.508	**58.52**	2926
6.707	13.414	**58.38**	2919
8.126	16.252	**58.22**	2911
9.504	19.008	**58.04**	2902
10.839	21.678	**57.83**	2892
12.126	24.252	**57.61**	2881
13.363	26.726	**57.37**	2869

Table 2 – Effective area of the beam entering in the prismatic lens as a function of the entrance angle, with a = 50 mm.

For the determination of P_{out} it is necessary to distinguish the two types of secondary optics.

For the reflection concentrator, the PV receiver is placed on the exit aperture and it collects all the light coming from it. Therefore, in this case P_{out} is obtained by integrating all the radiation collected in the scan.

For the lens, the PV receiver is placed at 5 cm distance. It will collect the light that falls directly on it and that is reflected from the lateral flaps. P_{out} is then obtained as the sum of these two contributions. The situation is illustrated in Figures 5 and 6. The radiation within the red rectangle is coming directly from the lens, while the radiation inside the yellow rectangles is reflected by the flaps. In any case, from the pictures of focused beam it can be noted that the light falls predominantly within the central band.

It is interesting to examine the values of efficiency and concentration obtained for the individual angles. The collection efficiency η_i is calculated using Eq. (1) while the concentration factor C_i is obtained from Eq. (4). Tables 3, 4 and 5 illustrate the results corresponding to each angle β_i (mirror tilt from the mirrors line); the columns report entrance angle α_i', collection efficiency η_i and concentration factor C_i.

β_i (°)	α_i' (°)	η_i	C_i
0.759	1.518	0.717	3.75
2.273	4.546	0.708	3.71
3.774	7.548	0.701	3.67
5.254	10.508	0.695	3.64
6.707	13.414	0.674	3.53
8.126	16.252	0.657	3.44
9.504	19.008	0.638	3.34
10.839	21.678	0.613	3.21
12.126	24.252	0.589	3.08
13.363	26.726	0.548	2.87

Table 3 – Collection efficiency and concentration factor varying the tilt angle, for the reflection concentrator.

β_i (°)	α_i' (°)	η_i	C_i
0.759	1.518	0.749	5.25
2.273	4.546	0.752	5.26
3.774	7.548	0.745	5.21
5.254	10.508	0.744	5.21
6.707	13.414	0.750	5.25
8.126	16.252	0.740	5.18
9.504	19.008	0.712	4.99
10.839	21.678	0.697	4.88
12.126	24.252	0.667	4.67
13.363	26.726	0.614	4.29

Table 4 – Collection efficiency and concentration factor varying the tilt angle, for the first sample of prismatic lens (Lens1).

β_i (°)	α_i' (°)	η_i	C_i
0.759	1.518	0.744	5.21
2.273	4.546	0.753	5.27
3.774	7.548	0.756	5.29
5.254	10.508	0.755	5.29
6.707	13.414	0.739	5.17
8.126	16.252	0.736	5.16
9.504	19.008	0.728	5.10
10.839	21.678	0.699	4.89
12.126	24.252	0.686	4.80
13.363	26.726	0.593	4.15

Table 5 – Collection efficiency and concentration factor varying the tilt angle, for the second sample of prismatic lens (Lens2).

Finally the total values are obtained by summing the contributions of all the examined angles, as Eq. (3) and Eq. (5) indicate.

Tables 6 summarizes the values of total collection efficiency and total concentration factor for all the examined samples of secondary optics designed for the solar plant with Fresnel mirror configuration. For the prismatic lenses two situations are considered, assuming that the reflectance of the lateral flaps could be equal to 90% or 75%, for helping to understand the influence of the flaps in the resulting performance of the component.

Secondary collector	**Reflection of the flaps R (%)**	**total collection efficiency η**	**total concentration factor C**
Reflection concentrator		0.656	3.43
Lens1	90	0.695	4.87
Lens1	75	0.663	4.64
Lens2	90	0.696	4.87
Lens2	75	0.664	4.65

Table 6 – Total values of collection efficiency and concentration factor for all the examined secondary optics.

1. Analysis in the image plane

The distribution of the radiation concentrated on the image plane of the secondary collector is accurately analysed to assess the level of uniformity of receiver illumination. The images in Figures 4-6 are obtained elaborating the measurements with the photodiode, and provide a schematic representation of the illumination produced by the 20 mirrors. The contributions of the various mirrors are calculated by summing the acquired maps and their specular copies (added in the elaboration phase).

The image of the reflection concentrator (Fig. 4) is simply obtained by summing the contributions of the various angles, given that it was possible to align the photodiode with the exit aperture of the reflection concentrator, and thus the analysed area was always the same.

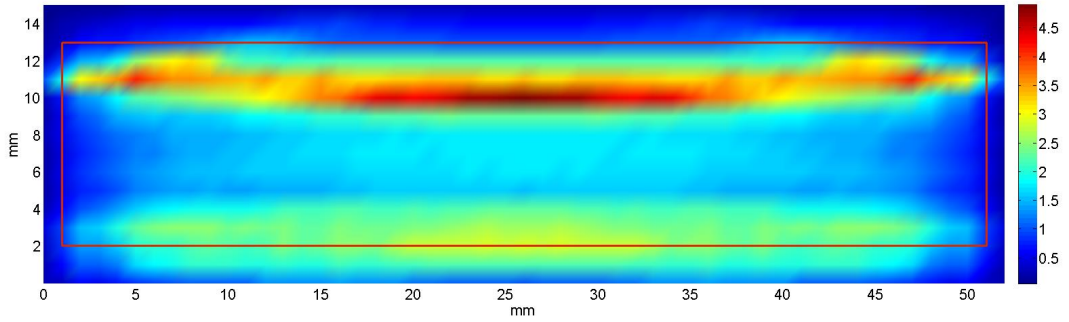

Fig. 4 – Elaboration in false colour of the power density (arbitrary units) on the image plane for the reflection concentrator.

The red rectangle in Fig. 4 denotes the area covered by the PV cell. It must be noted that this is not exactly the map of power density on the cell plane, because the measurement plane for Fig. 4 is about 2 mm behind it. Even

the light external to the rectangle is actually captured by the cell and contributes to the collection efficiency. The difference in intensity of the two horizontal bands at the edges of the rectangle can be attributed to a small vertical misalignment.

In Figures 5 and 6, in addition to the red rectangle of the cell, two side areas bounded by yellow lines are highlighted. The light that falls within these zones interacts with the lateral flaps of the collector and falls (attenuated) within the cell. For the evaluation of the collection efficiency it has been considered the contribution of the entire central band (with red zone and yellow zones). How the yellow zones contribute to the uniformity of illumination, however, depends on the interaction of the radiation with the flaps.

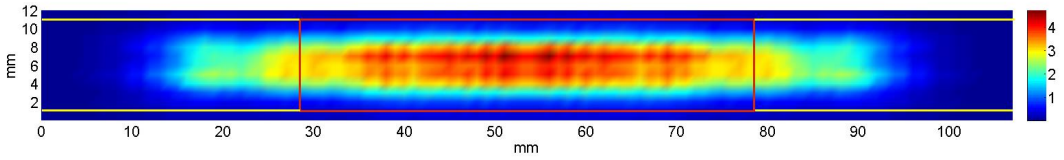

Fig. 5 – Elaboration in false colour of the power density (arbitrary units) on the image plane for Lens1.

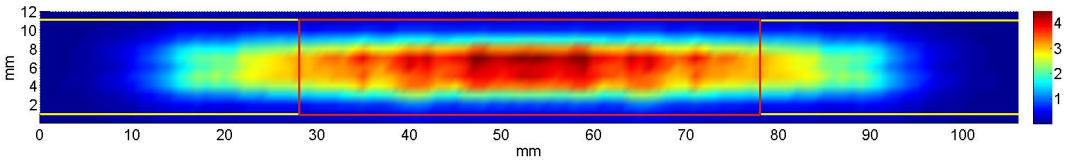

Fig. 6 – Elaboration in false colour of the power density (arbitrary units) on the image plane for Lens2.

The analysis is completed by the elaboration of the CMOS camera acquisitions. Due to the large size, the acquired images must be numerous and they must be accurately combined in order to obtain a final view of the illumination distribution.

As qualitative estimation, Figures 7 and 8 show the reconstructed images for reflection concentrator and prismatic lenses, respectively. Since fundamentally both lenses generate similar images, Fig. 8 shows only one image. It can be noted that the obtained images are in agreement with the results found with the photodiode.

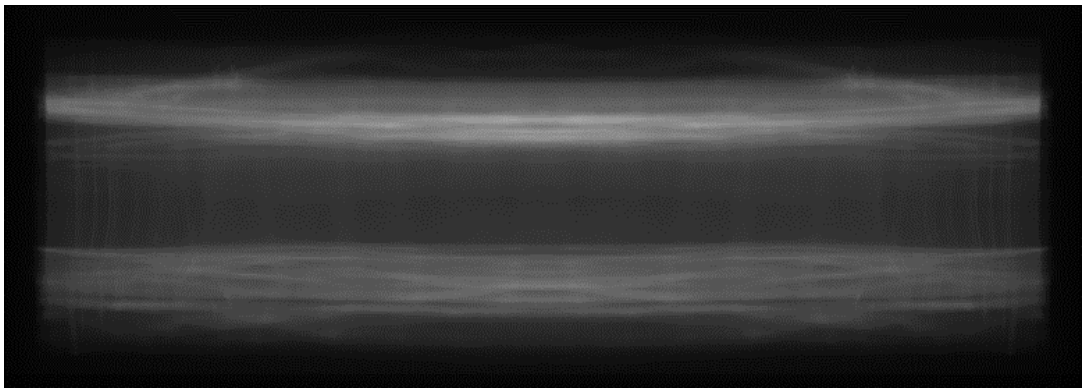

Fig. 7 – Image reconstructed for the reflection concentrator.

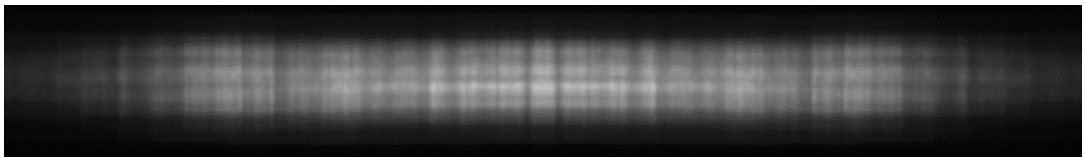

Fig. 8 – Image reconstructed for the prismatic lenses.

These reconstructed images serve only to have an idea of the distribution of the concentrated beam, which as it

can be seen in both cases is not homogeneous.

2. Conclusion

The purpose of this experimental work is to analyse the behaviour of two different secondary optics mounted near the focus of a solar collection system with a Fresnel mirror. An accurate analysis of the concentration layout and of the behaviour of the components inside the plant offered the possibility of performing in laboratory all the measurements simulating the behaviour of the single parts of the system. The contributions are then suitably combined to obtain collection efficiency and concentration factor of the entire solar plant.

The examined secondary optics are a prismatic lens and a reflection concentrator. These two types of secondary collector were optically designed for this solar plant, and samples of them were implemented. The tested secondary collectors are compared on the basis of their optical characteristics. The entrance area of the prismatic lens is larger than that of the reflective concentrator. The main comparison concerns total collection efficiency and total concentration factor of the secondary collector. These quantities are fundamental to understand the operation of the optical component and of the whole system for sunlight collection. The collection configuration is quite complicated and contains a large number of optical elements; therefore it was necessary to develop a special system for the calculation of collection efficiency and concentration factor. Another essential quantity to be analysed is the light distribution in the image plane of the secondary optics, because the level of uniformity of receiver illumination influences the photovoltaic conversion.

A specific experimental set-up was optically designed, implemented and aligned to perform the optical tests simulating the collection geometry of the existent plant. Having chosen to study the system at noon, there is symmetry with respect to the central axis of the system, so only half of the 20 mirrors were reproduced in laboratory. The procedure consists in performing the tests separately simulating the illumination of each mirror, finally combining the measured results. It was decided to perform the analysis at noon, considering that this hour usually corresponds to the maximum solar irradiation. In the actual plant the mirrors move during the day, thus for examining other day times 20 measurements are required and the inclination angles must be properly selected.

Two samples of prismatic lens and one sample of reflection concentrator are compared with an optical characterisation considering the inclinations of the mirrors at noon. The values of total collection efficiency (η) are very similar for all examined samples and they are around 0.66 – 0.69. The total concentration factor (C) is 4.6 – 4.9 for the prismatic lenses and 3.4 for the reflection concentrator. The higher value of C measured on the lenses is probably due to a larger entrance area of the prismatic lens with respect the other optics. In particular, specific tests verified that for some angles the beam does not completely enter into the reflective concentrator. To study the lighting distribution in the image plane of the secondary collector, the power density was computed from the photodiode measurements and some image reconstructions were obtained from the CMOS acquisitions. All these pictures evidence a quite uniform illumination of the receiver; only the two horizontal extremes show lower illumination levels.

The final results of this optical comparison are that the collection efficiency is comparable among all examined samples, while the concentration factor is higher for the prismatic lenses. Therefore, taking into account also that the entrance aperture of the prismatic lenses is larger with respect to the other, it can be concluded that the prismatic lens is a better performing secondary optics than the reflective concentrator. The characteristics of receiver illumination uniformity are analogous for both secondary collectors, which provide a focused image with elevated uniformity in the centre and some inferior light levels towards the right and left extremes.

Reminding that the presented study was carried out at noon, a more complete analysis should examine other hours of the day. Another interesting investigation could consider the angular limitations in order to control the losses, because the experimentation evidenced that there are some cases in which the reflection concentrator is not entirely illuminated.

3. References

Abbas, R., Montes, M.J., Piera, M., Martinez-Val, J.M., 2012. Solar radiation concentration features in Linear Fresnel Reflector arrays. Energy Conversion and Management 54, 133-144. (a)

Abbas, R., Muñoz, J., Martínez-Val, J.M., 2012. Steady-state thermal analysis of an innovative receiver for linear Fresnel reflectors. Applied Energy 92, 503-515. (b)

El Gharbi, N., Derbal, H., Bouaichaoui, S., Said, N., 2011. A comparative study between parabolic trough collector and linear Fresnel reflector technologies. Energy Procedia 6, 565-572.

Fernandez-Garcıa, A., Zarza, E., Valenzuela, L., Perez, M., 2010. Parabolic-trough solar collectors and their applications. Renewable and Sustainable Energy Reviews 14, 1695-1721.

Fontani, D., Sansoni, P., Sani, E., Coraggia, S., Jafrancesco, D., Mercatelli, L., 2013. Solar divergence collimators for optical characterisation of solar components. International Journal of Photoenergy 2013, 610173, 1-10.

Fontani, D., Sansoni, P., Francini, F., Jafrancesco, D., 2015. Comparison of two secondary optics for a Fresnel mirror. Proceedings of SolarPaces2015 – Cape Town, South Africa.

Kalogirou, S.A., 2004. Solar thermal collectors and applications. Progress in Energy and Combustion Science 30, 231-295.

Mills, D.R., Morrison, G.L., 2000. Compact linear Fresnel reflector solar thermal powerplants. Solar Energy 68, 3, 263-283.

Singh, P.L., Ganesan, S., Yadav, G.C., 1999. Performance study of a linear Fresnel concentrating solar device. Renewable Energy 18, 409-416.

Winston, R., Miñano, J.C., Benítez, P., Shatz, N., Bortz, J.C., 2005. Nonimaging Optics. Elsevier Academic Press, Amsterdam.